# **ARTICLE**

# C-H functionalization reactions enabled by hydrogen atom transfer to carbon-centered radicals

Received 00th January 20xx, Accepted 00th January 20xx

DOI: 10.1039/x0xx00000x

Sumon Sarkar, ‡a Kelvin Pak Shing Cheung, ‡a and Vladimir Gevorgyan\*a

Selective functionalization of ubiquitous unactivated C—H bonds is a continuous quest for synthetic organic chemists. In addition to transition metal catalysis, which typically operates under two-electron manifold, a recent renaissance of radical approach relying on hydrogen atom transfer (HAT) process has led to the tremendous growth of the area. Despite several challenges, protocols proceeding via HAT are highly sought after as they allow for relatively easy activation of inert C—H bonds under mild conditions leading to a broader scope and higher functional group tolerance and sometimes complementary reactivity over the methods relying on traditional transition metal catalysis. A number of methods operating via heteroatom-based HAT have been extensively reported over the past few years, while the methods employng more challenging carbon analogues have been less explored. Recent developments of mild methodologies for generation of various carbon-centered radical species enabled their utilization in the HAT process, which, in turn, led to the development of remote C(sp³)—H functionalization reactions of alcohols, amines, and amides and related compounds. This review covers mostly recent advances in C—H functionalization reactions involving HAT step to carbon-centered radicals.

#### Introduction

Selective functionalization of C–H bonds in organic molecules is highly desirable as this atom- and step-economic approach allows for late stage functionalization and diversification of complex molecules, and sometimes previously unattainable unique retrosynthetic disconnections.¹ However, selective and efficient functionalization of ubiquitous C–H bonds is a highly challenging task due to the inertness of these bonds, and also lack of control for activation of a specific C–H site among other similar C–H bonds available.²

Over the past decades, transition metal-catalyzed C–H activation and carbene/nitrene insertion reactions have been developed tremendously (Scheme 1a).<sup>3</sup> However, these methods typically require high temperature conditions, as well as directing groups, some of which are not removable. The selectivity of C–H activation mostly depends on thermodynamic stability of the resultant carbon-metal species. Thus, primary C–H sites are easier to activate compared to their secondary counterparts; whereas activation of tertiary C–H bonds are rare. On the other hand, carbene and nitrene insertion reactions occur preferentially at the most electron-rich C–H bonds. Nonetheless, steric influence can be the dominant factor in some cases. Moreover, these processes usually employ diazo compounds or amides to access the corresponding metal carbene and metal nitrene species. An electron withdrawing

In contrast, hydrogen atom transfer (HAT),<sup>4</sup> represents an alternative approach toward C–H functionalization. Since HAT is highly influenced by bond dissociation energy (BDE), for a given system, HAT from tertiary C–H sites are faster HAT than that from secondary and primary positions. Thus, methods relying on HAT exhibit selectivity trend complementary to that for two-electron transition metal-catalyzed approaches.<sup>5</sup>

HAT process has long been recognized as a versatile tool for C–H functionalization for its high reactivity and regioselectivity. Historic precedence of 1,5-HAT initiated by nitrogen- and oxygen- centered radicals was showcased in Hofmann-Löffler-Freytag reaction and Barton's nitrite photolysis.<sup>6</sup> This radical approach discovered in 19th century, despite being highly regioselective and exergonic, did not make appearnce in the mainstream of C–H functionalization methods until mild generation of radicals have been developed.<sup>7</sup> Likewise, carbon-centered radical-mediated HAT was first reported in 1954<sup>8</sup> and have not been utilized in organic synthesis until late 1980's,<sup>9</sup> however enjoyed rapid employment in synthesis in the past decade.

Rate of HAT is mostly controlled by enthalpic factors, however Thrope-Ingold effect also plays an important role in case of intramolecular HAT.<sup>10</sup> With few exceptions,<sup>11</sup> HAT proceeds via early transition state due to its exothermic nature. Usually aryl, vinyl, or primary alkyl radicals undergo HAT at alkyl C–H sites due to their higher parent C–H BDEs (Scheme 1, b(i)). In the case where these BDE differences are comparable, the process can potentially be reversible,<sup>12</sup> thus a selective functionalization

group such as ester (i.e.  $\alpha$ -diazo ester) is often required, thus limiting the choice of reaction substrates.

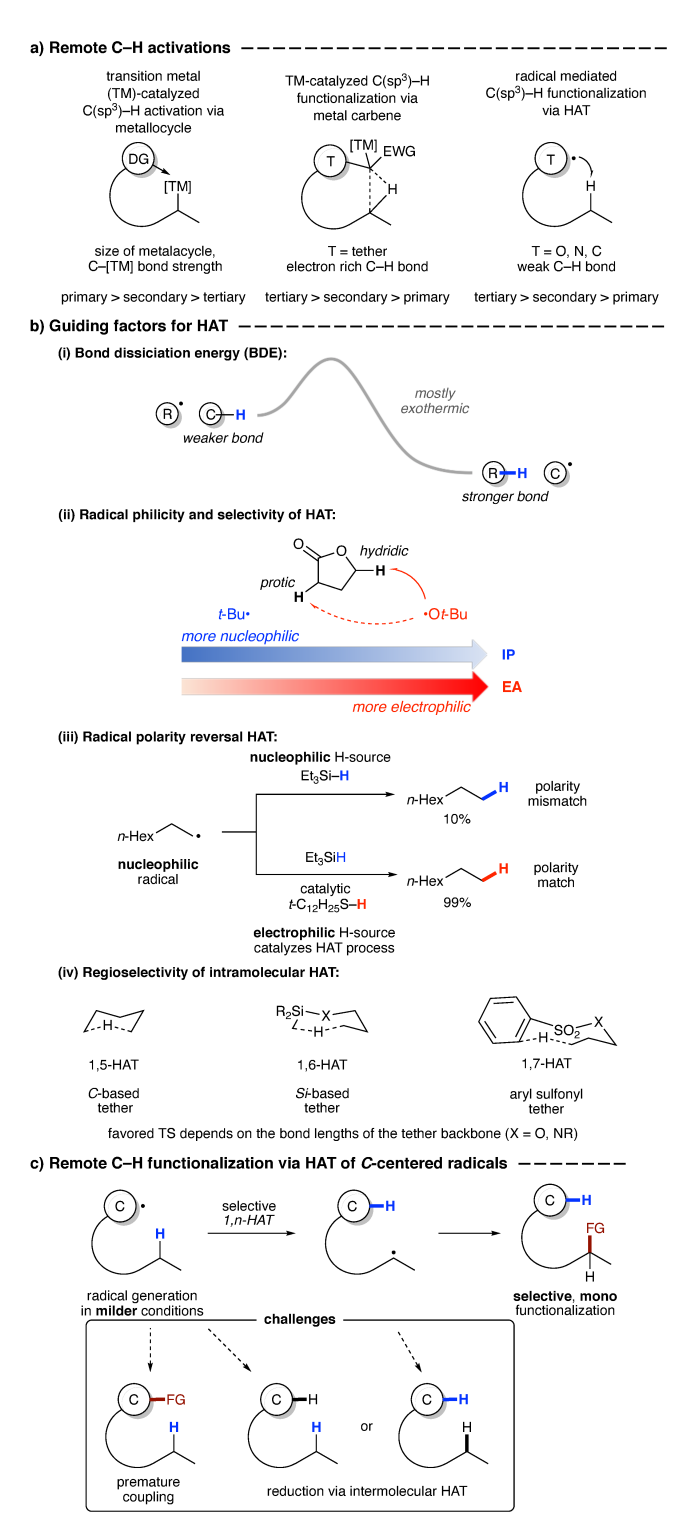
Department of Chemistry and Biochemistry, University of Texas at Dallas, 800 W Campbell Rd, Richardson, Texas, 75080, USA. E-mail: vlad@utdallas.edu.
 ‡These authors contributed equally to this work.

becomes more challenging. Another important factor governing efficiency and selectivity of HAT is radical philicity (polarity). <sup>13</sup> Radical philicity, electrophilicity-, or nucleophilicity index can be quantified from ionization potential (IP) and electron affinity (EA) of free radicals. Given similar BDE differences, an electrophilic radical is expected to undergo HAT preferentially from more hydridic C–H site and vice versa (b(ii)). <sup>4b,14</sup> In case of polarity mismatch, another HAT agent can be used for polarity reversal catalysis (b(iii)). <sup>15</sup>

*C*-centered radicals can abstract hydrogen via intramolecular 1,n-HAT where n=4-8, or even beyond (b(iv)). $^{7a,b,7d-g}$  The predictable site-selective HAT relies on optimal orientation (linear to quasi-linear:  $\leq 35^{\circ}$ ) and distance ( $\leq 3$  Å) between radical and the H-atom at the abstraction site. $^{16}$  Higher activation energy for other intramolecular HAT can be attributed to increased C–H–C strain for 1,3 and 1,4-HAT, or entropic barrier for higher order HATs. However, incorporation of heteroatoms can alter the preferred geometry and thus the site of HAT. For example, silicon-based tether displays a preference for 1,6-HAT, while arylsulfonyl tether is predisposed to 1,7-HAT (see below).

Commonly generation of O- and N-centered radicals for HAT involve single electron reduction of very weak oxygen- or nitrogen-heteroatom bonds or strong oxidants required to oxidize nitrogen or oxygen centers. On the contrary, generation of C-centered radicals can now be done under variety of benign conditions using organic halides, redox-active esters, triflates, and diazonium salts. However, there are few challenges associated with the C-H functionalization via HAT of C-centered radicals (Scheme 1c). Since both initial- and translocated radical are very similar in nature, there is a possibility for premature coupling process. However, this problem can be addressed by using radicals of different radical philicities and by matching polarity of the reagent and translocated radical.<sup>17</sup> In addition, due to lower BDE differences, the rate of HAT to C-centered radical from alkyl C-H site can be low, thus competing with other HAT processes, including unwanted intermolecular HAT process with solvent giving rise to reduction byproducts.

This review covers C–H functionalizations involving HAT to *C*-centered radical, with emphasis placed on theoretical background and challenges of HAT involving *C*-centered radicals. It should be noted that this topic has been partially covered in several excellent reviews,<sup>5,7a-d</sup> however since then increasing number of reports have appeared in literature. Hence, this review summarizes the progress in this emerging area of HAT, organized by the distance of HAT and type of *C*-centered radical.



**Scheme 1** (a) Different modes of remote C–H functionalizations. (b) Guiding factors for HAT. (c) Remote C–H functionalizations via HAT to *C*-centered radicals.

# HAT Involving Alkyl Radicals Intramolecular HAT

#### 1,4-HAT

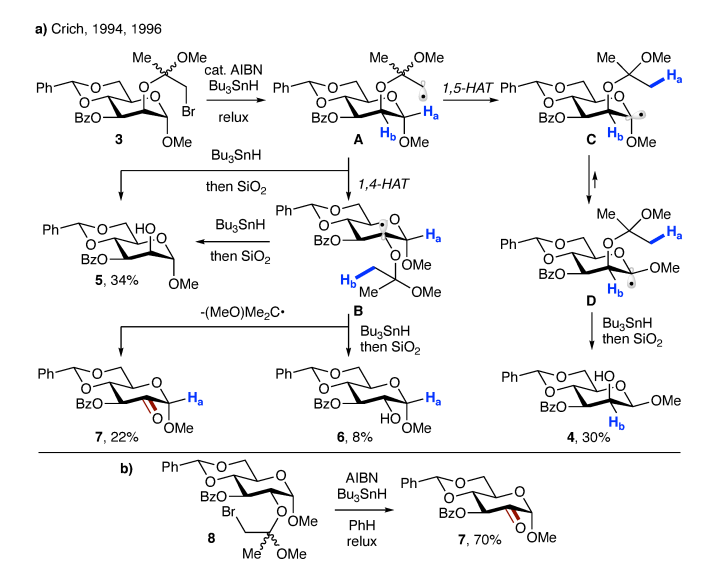
Literature examples of 1,4-HAT are scarce and typically involve sterically constrained substrates. Hart and co-workers observed oxindole  ${\bf 2}$  as the major product during their studies toward synthesis of the oxindole fragment of gelsemine (Scheme 2). Use of tributyltin deuteride led to product  ${\bf 2}$ -D, thus supporting the mechanism in which intermediate  ${\bf A}$ , formed upon radical cyclization of bromide  ${\bf 1}$  in the presence of tributyltin hydride (Bu<sub>3</sub>SnH) and azobisisobutyronitrile (AIBN) initiator, undergoes 1,4-HAT to give stable tertiary benzylic radical  ${\bf B}$ . In this case, 1,4-HAT is favored by not only enthalpic factor but also rigidity of  ${\bf A}$ , which ensures the radical center to be in close proximity to  ${\bf H}_a$ .

Scheme 2 1,4-HAT in synthetic studies toward gelsemine.

Crich and co-workers showed that 1,4-HAT could be a competitive pathway during the inversion of  $\alpha$ - to  $\beta$ -pyranosides via 1,5-HAT.<sup>19</sup> As depicted in Scheme 3a, reaction of **3** with Bu<sub>3</sub>SnH in the presence of AIBN leads to radical **A**, which can undergo 1,5-HAT, followed by axial HAT, to afford desired  $\beta$ -mannoside **4** after workup. Alternatively, competing 1,4-HAT can occur, resulting in intermediate **B**. The latter may afford  $\alpha$ -mannoside **5** or glucoside **6** via HAT, or ketone **7** upon  $\beta$ -scission. Product distribution clearly shows that 1,4-HAT is not only viable but indeed the major pathway in this rigid system. In addition, exclusive formation of ketone **7** was observed when glucoside **8** was used (Scheme 3b).

In 2001, Zard and Cassayre reported short synthesis of (–)-dendrobine, $^{20}$  in which the pyrrolidine core was thought to be constructed via radical cyclization of the corresponding trichloroacetamide (9  $\rightarrow$  10, Scheme 4a). However, upon treatment of model substrate 9 with nickel and acetic acid in the presence of diphenyl diselenide, enamide 11 was obtained

instead of the anticipated bicyclic lactam **10**. This suggests that 1,4-HAT toward stable allylic radical **B** occurred preferentially



**Scheme 3** (a) 1,4-HAT triggered by radical **A** originated from bromoethyl mannoside **3**. (b) Synthesis of ketone **7** by 1,4-HAT/fragmentation of bromoethyl glucoside **8**.

over the 5-exo-trig cyclization. Bertrand, Nechab and coworkers provided a plausible explanation based on the conformational analysis of conformers **A-1** and **A-2** leading to 1,4-HAT and 5-exo-trig processes, respectively (Scheme 4b).<sup>21</sup>

**Scheme 4** (a) Formation of cyclic enamide **11** via 1,4-HAT/arylselenation cascade. (b) Conformational analysis for 1,4-HAT process vs 5-*exo-triq* cyclization.

Ryu and co-workers observed formation of three different products while investigating the reactivity of  $\alpha$ -ketenyl radicals with an internal amino group (Scheme 5a). The reaction begins with radical addition of tributyltin radical to 12, followed by trapping of carbon monoxide to give  $\alpha$ -ketenyl radical A, which then engages in nucleophilic cyclization with tethered amino group. A subsequent proton transfer affords hydroxylallyl radical B, which may either be oxidized to lactam

13, convert to reduced lactam 14 upon intermolecular HAT with  $Bu_3SnH$ , or perform 1,4-HAT to produce intermediate  $\bf C$ . The latter then extrudes tributyltin radical to furnish 15. Alternatively, 15 could be obtained via protodestannylation of 13, as exemplified in the one-pot two-step transformation of 12c to 15c. Products distribution varies with the lactam ring size, with larger rings favoring 1,4-HAT over the other two pathways. This was later rationalized by DFT calculations, which showed that despite all being highly exothermic, activation barrier decreased with ring size (17.0 kcal/mol for n = 4 vs 25.3 kcal/mol for n = 1).  $^{22b}$  It was also found that in the case of phenethylamines 16, ejection of phenethyl radical preceded proton transfer and hence bypassed 1,4-HAT, resulting in intermediate  $\bf A$ , which was exclusively converted to  $\bf B$ , which upon treatment with TMSCI afforded lactam 17 (Scheme 5b).

**Scheme 5** (a) Rationale for the formation of three products. (b) Phenethyl radical as a leaving group.

In 2006 and 2008, Dake and co-workers disclosed synthetic routes toward nitiol derivatives **20**<sup>23</sup> and fusicoccane A–B ring fragment **21**<sup>24</sup> involving tandem Norrish type 1 fragmentation/1,4-HAT (Scheme 6). First, upon UV irradiation, a photoexcited ketone **18** undergoes fragmentation to form biradical **A**, which after intersystem crossing (ISC) performs 1,4-HAT to afford ketene intermediate **B**. Nucleophilic trapping with methanol solvent leads to the key intermediate, ester **19**.

**Scheme 6** Synthesis of natural product derivatives **20** and **21** via 1,4-HAT process.

In 2012, groups of Li and Shi reported synthesis of bicyclo[3.1.0]hexane derivatives 22 via radical reaction between vinylidene cyclopropanes and diphenyl diselenide.<sup>25</sup> The vinylcyclopropane moiety of 22 undergoes thermally-induced ring-opening, followed by 1,4-HAT, to give biradical C, which produces cyclohexene derivatives 23 or 24 (Scheme 7a). In all cases, excellent stereoselectivity was observed, which could be explained by unfavourable formation of the conformer B. Involvement of 1,4-HAT in this thermal rearrangement was supported by reaction of D-labeled substrate 22c, as well as by DFT calculations (Scheme 7b).

**Scheme 7** (a) Thermally-induced ring-opening/1,4-HAT cascade transformation of **22**. (b) Evidence for 1,4-HAT process by deuterium-labelling experiment.

#### 1,5-HAT

Studies toward the chemistry of carbon-to-carbon 1,5-HAT date back to the 1970s. In 1973, Morrison group revealed that olefin **25** underwent UVC-photoinduced internal exchange between vinyl deuterium and methyl hydrogen (Scheme 8a).<sup>26</sup> UV excitation of **25** generates 1,2-biradical **A**, which undergoes 1,5-HAT to produce *o*-xylylene intermediate **B**, followed by ground state 1,5-deuterium shift to afford exchanged product **26**. Later, Pratt confirmed the intermediacy of *o*-xylylene in the formation of [4+2] adduct **28** with maleic anhydride (Scheme 8b).<sup>27</sup> Similar transformations have also been reported by Hornback.<sup>28</sup>

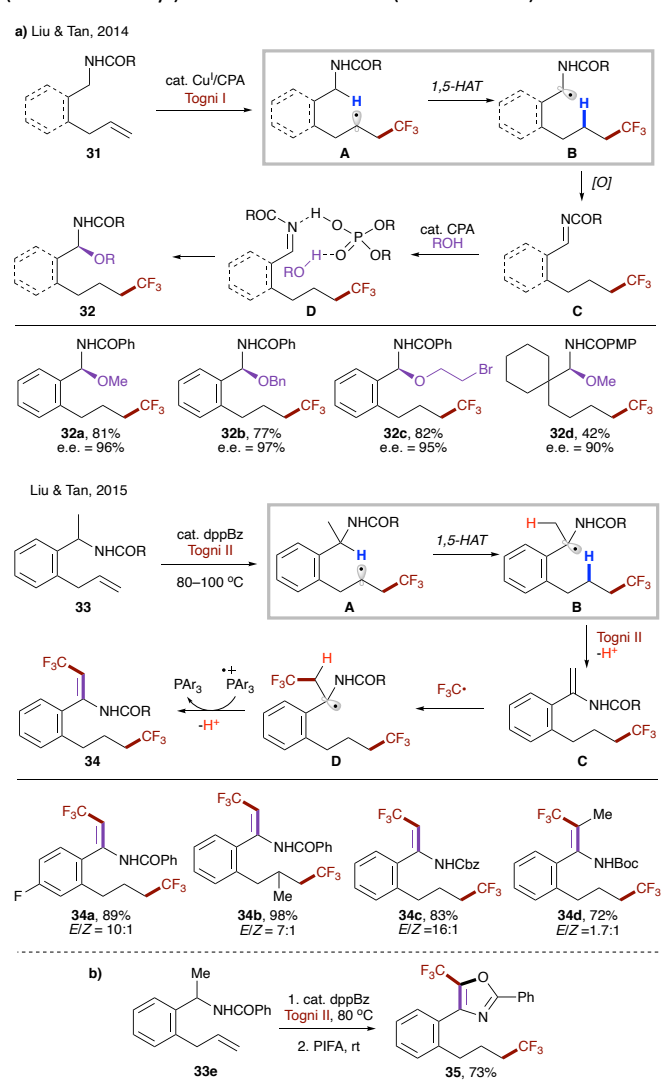
**Scheme 8** (a) Photoinduced internal H/D exchange of **25**. (b) Trapping of *o*-xylylene intermediate with maleic anhydride.

Very recently, Koert group reported an interesting example of naphthocyclobutene synthesis from methyl ( $\alpha$ -napthyl) acrylates **29**. <sup>29</sup> 1,2-biradical **A**, formed upon energy transfer (EnT) from photoexcited iridium catalyst, underwent 1,5-HAT to produce intermediate **B**. In contrast to the above cases, instead of the formation of o-xylylene, cyclobutane **30** is furnished after ISC/recombination of radicals. Thus, this transformation represents a carbon analogue of Norrish–Yang reaction. The performed reaction with deuterium-labelled substrate provided evidence for 1,5-HAT, as well as it being the rate-determining step (**30e**).

**Scheme 9** Synthesis of cyclobutanes **30** via EnT-induced 1,5-HAT to 1,2-biradical.

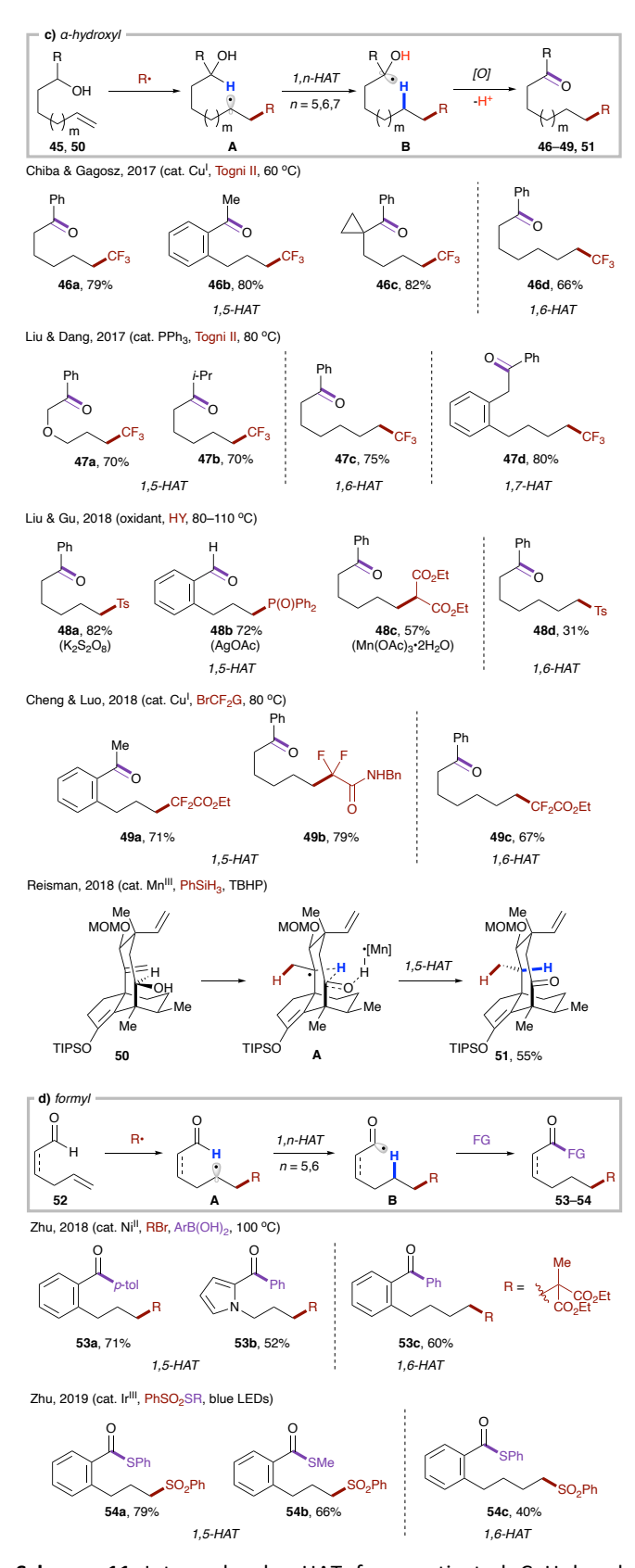
In 2014, Liu, Tan, and co-workers reported enantioselective C–H alkoxylation involving 1,5-HAT process (Scheme 10a). 30a Trifluoromethyl radical, formed upon single electron reduction of Togni's reagent by copper(I) catalyst, undergoes radical

addition to substrate 31. A subsequent 1,5-HAT occurs to form more stabilized  $\alpha$ -amido radical **B**, followed by a single electron oxidation to produce imine intermediate C. Finally, the nucleophilic attack of alcohol in the presence of chiral phosphoric acid (CPA) furnishes enantioenriched product 32. The authors also demonstrated a feasibility of HAT with aliphatic amide (32d). Later, a related transformation that also relied on 1,5-HAT was disclosed (Scheme 10a).30b In this case, catalytic amount of 1,2-bis(diphenylphosphino)benzene (dppBz) serves as single electron reductant and generates trifluoromethyl radical with Togni II reagent under thermal conditions. Similarly, radical addition to 33 leads to the more stabilized radical B. Electron transfer to another equivalent of Togni II reagent, followed by a proton loss leads to, in contrast to imine in the first report, enamide **C**, which is susceptible to another radical addition. Single electron oxidation followed by proton loss delivers the reaction product 34 and regenerates the phosphine catalyst, respectively. A one-pot procedure was also developed for synthesis of (trifluoromethyl)oxazoles such as 35 (Scheme 10b).



**Scheme 10** (a) Radical addition-triggered 1,5-HAT. (b) One-pot synthesis of 5-(trifluoromethyl)oxazole **35**.

A reaction mode where 1,5-HAT is induced by radical addition to a tethered double bond has proved to be efficient and general. Based on this strategy, transformations targeting weak C–H bonds, including benzylic (Scheme 11a), $^{31}$   $\alpha$ -carbonyl (Scheme 11b), $^{32}$   $\alpha$ -hydroxyl (Scheme 11c), $^{31a,33}$  and formyl (Scheme 11d), $^{34}$  have been developed. Notably, these substrates are also amenable to entropically less favored 1,6-and 1,7-HAT due to presence of radical-stabilizing groups.



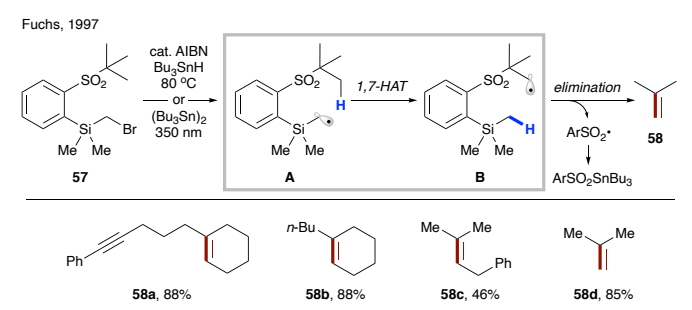
**Scheme 11** Intramolecular HAT from activated C–H bonds initiated by radical addition to tethered olefin. (a) Benzylic C–H. (b)  $\alpha$ -carbonyl C–H. (c)  $\alpha$ -hydroxyl C–H. (d) Formyl C–H.

Very recently, Wang and co-workers reported iron-catalyzed remote functionalization that operates in a similar fashion.<sup>35</sup> Remarkably, the catalytic system could be applied not only to activated systems, but also to unactivated ones (Scheme 12). Notably, substrate bearing secondary C–H site could also be employed (56c).

Scheme 12 Intramolecular HAT from unactivated C-H bonds.

#### 1,7-HAT

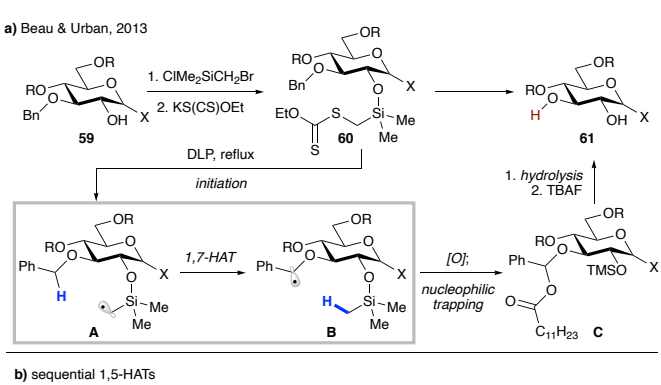
In 1997, Fuchs group disclosed examples of 1,7-HAT to C(sp³)-centered radicals (Scheme 13).³6 Under classical free radical conditions, (bromomethyl)silyl species 57 is converted to the corresponding silylmethyl radical **A**, which then engages in a 1,7-HAT process leading to the translocated radical **B**. A facile elimination of arylsulfonyl radical then affords olefin product 58. Both secondary (58a–c) and primary (58d) C–H sites were amenable to HAT giving good yields of alkenes, except for 58c due to competing abstraction of benzylic hydrogens. The uncommon 8-membered transition state for this HAT transformation can be attributed to the increased tether length possessing sulfur and silicon atoms. Mechanistic studies ruled out the possibility of intermolecular HAT event.

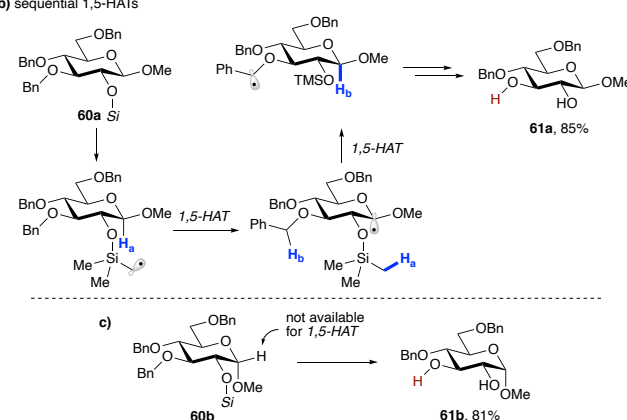


**Scheme 13** Formation of alkene via 1,7-HAT/ $\beta$ -elimination of **57**.

In 2013, Beau, Urban and co-workers reported selective monodebenzylation of benzyl-protected carbohydrate templates **59** that involved a key 1,7-HAT step triggered by silylmethyl radical (Scheme 14a).<sup>37</sup> The substrates were readily converted to the corresponding xanthate methylsilyl ethers **60** via a sequential silylation and substitution by xanthate. Thermal decomposition of dilauroyl peroxide (DLP) initiates the process to produce electrophilic silylmethyl radical intermediate **A**, which

undergoes 1,7-HAT to furnish benzylic radical **B**. Oxidation of the latter by DLP generates stable benzylic cation, which is trapped in the form of acyl acetal **C**. A subsequent hydrolysis and desilylation delivers the reaction product, diol **61**. In the case of  $\beta$  anomers such as **60a**, an alternative path could be operational, which involves a successive 1,5-HAT from anomeric C–H and then benzylic C–H sites (Scheme 13b). However, the authors discounted this possibility as  $\alpha$  anomer **60b**, which does not possess suitable hydrogen at the anomeric site, reacted smoothly to give **61b** with similar efficiency (Scheme 13c).





**Scheme 14** (a) Selective mono-debenzylation of **59**. (b) Plausible mechanism for sequential 1,5-HATs leading to the same product. (c) Validation of 1,7-HAT based on efficient debenzylation of **60b**.

Later in 2015, the groups of Zeng, Ren and Wu utilized 1,7-HAT process in the construction of isocopalane skeleton (Scheme 15). Radical precursor 63 was readily prepared from naturally abundant andrographolide 62. Upon heating, 63 undergoes homolytic cleavage of S–Cl bond and SO<sub>2</sub> extrusion leading to primary alkyl radical A. 1,7-HAT then follows, resulting in the more stable  $\alpha$ -acyloxy- or  $\alpha$ -alkoxy radical B. Finally, fragmentation of B affords the reaction product, aldehyde 64. Deuterium labelling studies confirmed the migration of hydrogen atom, thus ruling out a sequential 1,5-HAT (*vide supra*). Furthermore, catalytic amounts of benzoyl peroxide accelerated the reaction while TEMPO shut down the reaction, suggesting a radical pathway for this transformation. Several protecting groups R were examined, which led to moderate to

good yields (64a-d), with the exception of benzoylated substrate (64e). Interestingly, methyl ether was a viable substrate (64f).

Zeng, Ren & Wu 2015

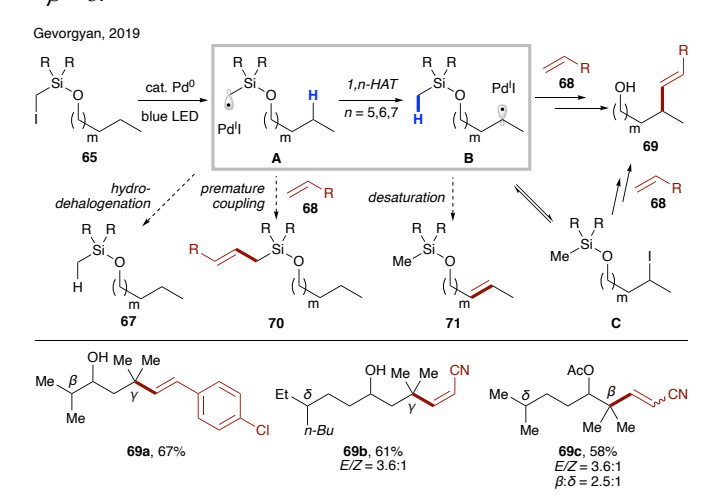
**Scheme 15** Construction of isocopalane framework **64** involving 1,7-HAT.

### **Intramolecular HAT at Competing Sites**

In 2017, Gevorgyan and co-workers demonstrated the ability of hybrid alkyl palladium-radical species to undergo selective intramolecular HAT at unactivated C(sp3)-H sites, featuring an easily installable/removable silicon-based auxiliary (Scheme 16).<sup>39</sup> Substrate **65**, readily accessible via routine silyl protection of the corresponding alcohol, engages in a single electron transfer (SET) with photoexcited Pd(0) catalyst to form hybrid radical A, which undergoes rate-limiting site-selective 1,n-HAT to produce translocated radical B. The latter may either recombine with Pd(I) followed by  $\beta$ -hydride elimination, or undergo direct HAT with Pd(I) to furnish remote desaturation product 66 after desilylation with TBAF. Side hydrodehalogenation process, which would produce reduced product 67, was suppressed under optimized conditions. This protocol allows for activation of both secondary and tertiary C(sp<sup>3</sup>)–H bonds at  $\beta$ -,  $\gamma$ -, and  $\delta$  sites (**66a–c**). Remarkably, high level of site-selectivity was maintained even with substrates bearing competitive sites with similar BDEs (66d-f). Kinetic studies suggested the selectivity preference to be 1,6-HAT ( $\gamma$ ) > 1,5-HAT ( $\beta$ ) > 1,7-HAT ( $\delta$ ). The preference of 1,6-HAT over the more common 1,5-HAT can be attributed to the increased tether length and flexibility of the tether possessing silicon atom.40 This method represents the first practical catalytic desaturation of aliphatic alcohols under mild, auxiliary-enabled, visible light-induced conditions.

**Scheme 16** Remote desaturation of aliphatic alcohols via selective 1,*n*-HAT enabled by iodomethylsilyl auxiliary.

Photoexcited palladium catalysis has been developed for alkyl Heck reaction and C–H activation,  $^{41}$  which had not been utilized synergistically to achieve more complex transformations. Very recently, Gevorgyan group disclosed site-selective radical Heck reaction relay of aliphatic alcohol derivatives **65** with various alkenes **68** to achieve alkenylation at remote unactivated  $C(sp^3)$ –H sites (Scheme 17). Potential side reactions, such as premature Heck reaction (**70**) and desaturation (**71**) were suppressed under optimized conditions. Interestingly, iodide **C** was observed over the course of reaction, which was shown to produce alkenol **69** under reaction conditions, thus suggesting its intermediacy in this transformation. As in the previous case (Scheme 16),  $^{39}$  this reaction exhibits the same site-selectivity:  $\gamma > \beta > \delta$ .



Scheme 17 Radical relay Heck reaction of aliphatic alcohols.

In continuation of employing silicon-based tethers for remote transformations, Gevorgyan group reported a transition metaland light-free directed amination of **65** (Scheme 18).<sup>16</sup> This method represents the first general approach for selective

amination of inert C(sp³)–H bonds at  $\beta$ -,  $\delta$ -, and  $\gamma$  sites. In the presence of lithium formate, readily available aryl diazonium salt **72** is reduced to generate aryl radical, which abstracts iodine atom from substrate. The resultant silyl methyl radical **A** is electrophilic and thus not predisposed to premature coupling with **72**. As such, desired 1,n-HAT occurs, leading to a transposed nucleophilic radical **B**, which undergoes facile radical addition to **72** to furnish diazenylation product **73**. It is noteworthy that primary C–H site is also reactive under the conditions of this method (**73d**). In addition, protected amino alcohols **74** can be obtained in reasonable yields via a one-pot three-step protocol.

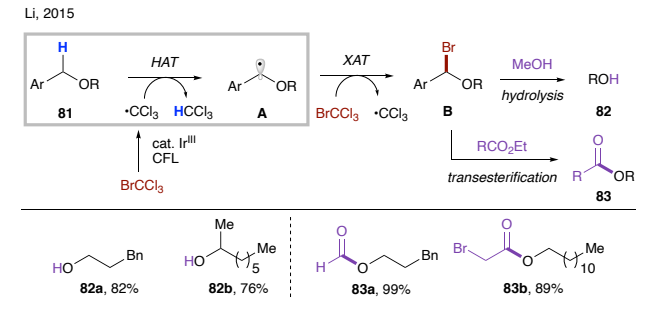
**Scheme 18** Transition metal- and light-free remote amination of aliphatic alcohols.

#### **Intermolecular HAT**

Efficient transformations involving intermolecular mediated by sp<sup>3</sup>-hybridized C-centered radicals are rare due to a smaller thermodynamic driving force, as compared to  $C(sp^2)$ -, N- or O-centered radicals. In 2002, Tomioka group utilized the instability of methyl radical to achieve intermolecular radical addition of ethers to aldimines (Scheme 19a).43 Dimethylzinc and oxygen initiate the reaction by producing methyl radical, which abstracts activated  $\alpha$ -hydrogen from ethereal solvent **76** to generate nucleophilic radical A. The latter then adds to aldimine 77 to give aminyl radical B, which is reduced by dimethylzinc to furnish product 78 after aqueous workup. Meanwhile, methyl radical is regenerated to close the radical chain cycle. Both cyclic and linear ethers are suitable substrates, albeit with moderate diastereoselectivity in most cases. Employment of diethylzinc and diisopropylzinc led to a drastic decrease in product yield due to significant formation of alkyl adduct 79 and/or reduction product 80, highlighting the pivotal role of methyl radical for efficient intermolecular HAT (Scheme 19b). Direct HAT between 76 and N-centered radical B is unlikely, as the reaction requires super-stoichiometric amount of zinc reagent. Later in 2003, the same group developed chemoselective addition of THF radical to aldehydes using  $Et_3B/air$  conditions.<sup>44</sup> This initiator-dependence was also applied to three-component reaction of aldehyde, amine and THF.

**Scheme 19** (a) Intermolecular HAT from **76** to methyl radical. (b) Superiority of methyl radical vs ethyl- and isopropyl radicals.

Given the relatively small thermodynamic driving force for the HAT step to the C-based radicals, the polarity match becomes an increasingly important factor. In 2015, the Li group reported visible light-promoted transesterification and debenzylation reactions of alkyl benzyl ethers **81** (Scheme 20). $^{45a}$  Trichloromethyl radical is first generated via a single electron reduction of bromotrichloromethane by photoexcited iridium catalyst. $^{46}$  A polarity-matched intermolecular HAT between this electrophilic radical and the electron-rich C–H bond in **81** occurs, resulting in nucleophilic radical **A**. A subsequent halogen atom transfer (XAT) produces  $\alpha$ -bromoether **B** and trichloromethyl radical, thereby propagating the radical chain process. Intermediate **B** can either be hydrolysed in methanol in a one-pot two-step manner to the debenzylation products **82** or undergo in situ transesterification to afford esters **83**.



**Scheme 20** Employment of trichloromethyl radical in intermolecular HAT.

Later, Li group showed that substrates possessing secondary benzylic C–H bonds (84) are also competent for analogous bromination, thus affording benzyl bromides 85 in good to excellent yields (Scheme 21a).<sup>45b</sup> In addition, a one-pot synthesis of benzyl amines 86 was developed, albeit huge excess of amine was required to achieve good yields. In 2019, Kappe and co-workers disclosed the same process for toluene

derivatives **87** under continuous flow reaction setup using benzophenone as photocatalyst (Scheme 21b).<sup>45c</sup> Moderate yields of benzylamines **89** were obtained when **87** was susceptible to dibromination (**89a**).

**Scheme 21** Benzylic C–H bromination *en route* to benzyl amines via intermolecular HAT. (a) Secondary benzylic C–H. (b) Primary benzylic C–H.

#### **HAT involving vinyl radicals**

Larger BDE difference between olefinic C-H (~110 kcal/mol) and aliphatic C-H (~96-100 kcal/mol) bonds renders the 1,n-HAT process more efficient compared to that by alkyl radical.<sup>47</sup> According to studies by Gilbert and co-workers, the rate of 1,5-HAT at activated C-H site by vinyl radical is more than 10<sup>5</sup> s<sup>-1</sup>.<sup>48</sup> After HAT process, usually alkene moiety serves as radical acceptor for the translocated radical, leading to the formation of cyclopentane or cyclohexane derivatives.<sup>49</sup> In general, vinyl radical is generated by halogen abstraction/single electron reduction of the corresponding vinyl halides or via radical addition to alkynes.50 The second approach is more attractive from practical standpoint, since the first protocol requires synthesis of vinyl halides. However, despite being exothermic in nature, the intermolecular radical addition to alkyne is a relatively slow process. The feasibility of HAT by vinyl radical was first reported in 1967 by Heiba and Dessau in the novel radical cascade involving addition of •CCl<sub>3</sub> across triple bond that triggered 1,5-HAT. $^{50b}$  However, it was not until 1988 when the first systematic studies on 1,5-HAT of vinyl radicals were reported by Parsons.9b

# Intramolecular HAT

#### 1.4-HAT

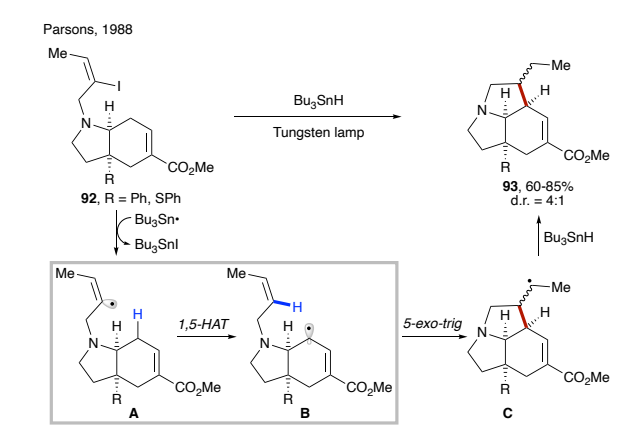
1,4-HAT of vinyl radical has been observed rarely, typically in sterically constrained substrates, usually as a side reaction. First 1,4-HAT was implemented by Malacria and co-workers in synthesis of enantiomerically pure 1,2,3-triols.<sup>51</sup>

**Scheme 22** Synthesis of steroidal core of batrachotoxin via 1,4-HAT of vinyl radical.

In 2016, Du Bois and co-workers achieved concise asymmetric synthesis of the natural (–) and non-natural (+) antipodes of batrachotoxin, as well as both enantiomers of a C-20 benzoate-modified derivative (Scheme 22).<sup>52</sup> The key radical cascade sequence involving 1,4-HAT of vinyl radical formed in situ is highly efficient and selective. The process commences with addition of tributyl tin radical at terminal alkyne of **90**, followed by sequential 6-endo-trig/5-exo-dig cyclizations to produce reactive intermediate **A**. This electrophilic radical then undergoes 1,4-HAT to form stabilized nucleophilic allylic radical species **B**, which is quenched by Bu<sub>3</sub>SnH to deliver **91** in 75% yield.

# 1,5-HAT

In 1988, Parsons group first demonstrated that vinyl radicals could undergo translocation to alkyl sites via intramolecular HAT (Scheme 23).9b In the presence of Bu<sub>3</sub>SnH and tungsten lamp irradiation, the vinyl radical **A** generated from vinyl iodide **92** undergoes 1,5-HAT to afford translocated allylic radical **B**. 5-exo-trig cyclization of the latter, followed by reduction efficiently leads to the desired pyrrolizidine ring system **93** as a mixture of epimers.



**Scheme 23** 1,5-HAT triggered by vinyl radical in synthesis of pyrrolizidine ring system.

In their seminal work, Curran group reported translocation of vinyl radicals via 1,5-HAT (Scheme 24a).9a Realising that C-H bonds, the most attractive and simplest 'radical precursor', could not be activated via intermolecular HAT by tin radical due to its significantly endothermic nature, they utilized Bu<sub>3</sub>SnH as an atom transfer agent to access vinyl radical A from 94. Efficient 1,5-HAT occurs to form translocated alkyl radical B, which is cyclized to produce cyclopentane derivatives 96 after reduction. A premature reduction of the vinyl radical via intermolecular HAT leads to the acyclic alkene byproduct 95. In 1993, Curran group disclosed the substituent effect on these type of 1,5-HAT transformations.<sup>53</sup> Although a few exceptions exist, the authors found correlation between the rate of 1,5-HAT and the BDE of the C(sp³)–H bond. They also found that the overall geometry of the moiety undergoing HAT was likely to have more impact than the particular substituent at the target C-H site.

In 2018, Gevorgyan group reported photoinduced palladium-catalyzed non-chain atom transfer radical cyclization (ATRC) at remote unactivated aliphatic C–H sites with similar type of substrates (Scheme 24b).  $^{54}$  The hybrid vinyl palladium-radical **A** undergoes 1,5-HAT process to generate the translocated radical **B**, which upon 5-*exo-trig* cyclization leads to the intermediate **C**. Finally, iodine atom transfer from the putative Pd(I)I affords iodomethyl carbo- and heterocyclic motifs **97**, thus contrasting with the reductive transformation by Curran. Notably, no formation of Heck-type products via  $\beta$ -hydrogen elimination of the radical intermediate **C** was observed.

**Scheme 24** (a) Free radical translocation via 1,5-HAT (b) 1,5-HAT of hybrid vinyl palladium radical intermediate.

As discussed above, the alternative way to form vinyl radicals involves addition of radicals to alkynes. In 1967, Heiba and Dessau observed 1,5-HAT of vinyl radical during addition of polyhalomethanes to terminal alkynes. <sup>55</sup> In 1993, Bachi and coworkers reported formation of vinyl radical **A** via addition of tributyltin radical at alkyne moiety of **98**. A subsequent 1,5-HAT, followed by 6-endo-trig cyclization and  $\beta$ -tin elimination produce delivers  $\beta$ -lactam **C** (Scheme 25). <sup>56</sup> Upon DBU-catalyzed isomerization of double bond, methyl 1-oxahomoceph-4-em-5-carboxylate **100** was obtained in 40% yield, along with 25% of reduction byproduct **99**.

**Scheme 25** 1,5-HAT of vinyl radical in synthesis of bicyclic  $\beta$ -lactam.

Few years later, Malacria group reported an efficient radical cascade reaction for diastereoselective synthesis of highly functionalized cyclopentanes (Scheme 26a). In this transformation, substrate **101** forms  $\alpha$ -silyl radical upon XAT, which then cyclizes to give vinyl radical species **A**. 1,3-allylic interaction in *E*-**A** and eclipsed interaction between methyl and isopropyl groups in *Z*-**A2** render them less favourable conformers than *Z*-**A1**. The latter undergoes highly regioselective 1,5-HAT at unactivated C(sp³)—H site, leading to primary alkyl radical intermediate **B**. A following rarely observed 5-endo-trig cyclization constructs the cyclopentane moiety. Finally, the cleavage of the siloxy ring with MeLi affords product **102** in impressive 74% overall yield.

Recently, Dénés group disclosed the involvement of 1,5-HAT in a similar type of reaction sequences during synthesis of polysubstituted  $\gamma$ -butenolides (Scheme 26b). The deuterium labelling experiments revealed an "invisible" 1,5-HAT to the formed vinyl radical from aliphatic side chain. Expectedly, due to the greater stability of tertiary radical, the higher deuterium incorporation was observed in **104c**.

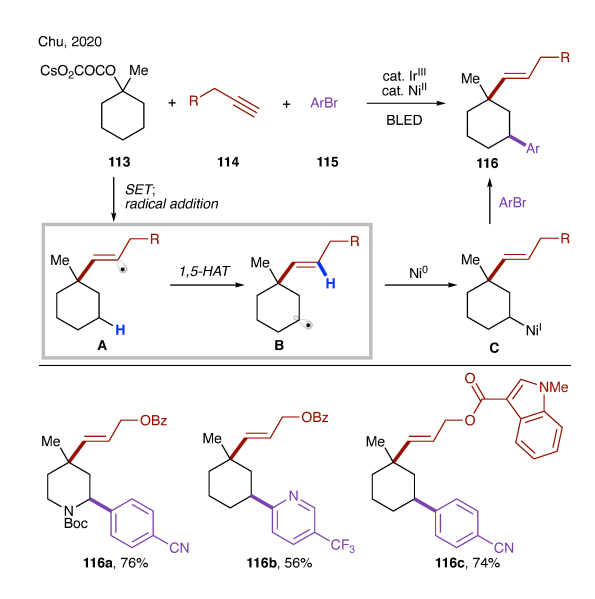
**Scheme 26** (a) Diastereoselective 1,5-HAT event triggered by 5-exo-dig cyclization, followed by 5-endo-dig cyclization. (b) 5-exo-dig cyclization followed by "invisible" 1,5-HAT.

In 2019, Zhu and co-workers reported mild, photocatalytic methods for activation of  $\delta$  C(sp³)–H bonds via formation of vinyl radicals (Scheme 27a). In both cases, the authors synthesized the tertiary propargyl alcohol derivatives **107** via addition of acetylide **106** at ketone **105**. Under the reaction conditions, the excited photocatalyst undergoes SET to generate electrophilic radical Y•, which adds to alkyne to trigger 1,5-HAT event. The translocated radical species **B** undergoes a sequence of 5-*exo-trig* cyclization,  $\beta$ -elimination and oxidation by photocatalyst to afford the final product **108–109**. Using this protocol, valuable, complex fluoroalkylated alkenes **108a–c**, <sup>59a</sup> and sulfonylvinylation products **109a–c**59b were easily accessed.

**Scheme 27** (a) Regioselective vinylation via 1,5-HAT, triggered by radical addition to alkyne. (b) Remote C–H functionalizations of alkyne via 1,5-HAT of vinyl radical formed by  $\beta$ -radical addition.

Recently, Li, Zhu and co-workers reported remote functionalization of heteroalkyne **110** via HAT of vinyl radical formed by β-radical addition (Scheme 27b).<sup>60</sup> The method involves addition of perfluoroalkyl radical to alkyne to generate vinyl radical **A**, which undergoes 1,5-HAT to produce nucleophilic alkyl or benzyl radicals **B**. In the first scenario, the translocated radical **B** is oxidized selectively to ketone or alcohol **111a–c**. Whereas in the second case, the radical **B** is trapped by electrophilic alkyne to afford remote alkynylation products **112a–c**.

Very recently, Chu group developed photoredox/nickel dual-catalyzed conditions for sequential deoxygenative vinylation/C—H arylation of tertiary oxalates (Scheme 28).<sup>61</sup> This multicomponent cascade is initiated by a single electron oxidation of oxalate **113** by photoexcited iridium catalyst, which results in decarboxylation, followed by addition of the formed tertiary alkyl radical to alkyne **114** to form vinyl radical **A**. The succeeding 1,5-HAT affords a translocated secondary alkyl radical **B**, which is captured by Ni(0) to form alkyl Ni(I) species **C**. The reaction product **116** is obtained upon nickel-mediated cross-coupling with aryl halide.



**Scheme 28** Photoredox/nickel dual-catalyzed radical cascade involving 1,5-HAT of vinyl radicals.

## 1,6-HAT

In 1998, Malacria and co-workers demonstrated an impressive cascade polycyclization toward efficient and highly diastereoselective assembly of triquinane core that features five radical cyclizations and one 1,6-HAT step (Scheme 29).  $^{62}$  In the presence of AIBN and Bu<sub>3</sub>SnH, formation of silyl methyl radical triggers the radical cascade, delivering **A** via successive 5-exo-dig and 5-exo-trig cyclization, followed by a rare 3-exo-trig and 5-exo-dig cyclizations to generate  $\alpha$ -silyl vinyl radical **B**. The latter undergoes 1,6-HAT at silylmethyl C(sp³)–H site to form primary silylmethyl radical, which upon cyclization followed by  $\beta$ -silyl elimination affords the product **118** in 66% yield.

**Scheme 29** Highly diastereoselective 1,6-HAT in synthesis of triquinane derivatives.

Several examples of radical cascade reactions showcased formation of electrophilic vinyl radical A generated from 119, which undergoes 1,6-HAT to form nucleophilic lpha-heteroatomic radical B. A subsequent 5-exo-trig cyclization, followed by reduction of forming alkyl radical affords the cyclic product 120 (Scheme 30). In 2002, Parsons and co-workers utilized this strategy to synthesize 122, the precursor of mitomycin ring systems.<sup>63</sup> Few years later, Reiser group reported synthesis of 2,3-disubstituted dihydrobenzofurans 125a-d involving similar type of 1,6-HAT process.<sup>64</sup> In 2017, the same group employed photoredox catalysis to synthesize 2,3-disubstituted indolines 127 using similar strategy. 65 Beaudy and co-workers also utilized this 1,6-radical translocation strategy to construct the central indoline core of several natural products (129, 130).66 In 2007, Yoshimura, Takahata, and co-workers reported synthesis of 6,5'-C-cyclouridines tris(trimethylsilyl)silyl (supersilyl) radical initiates the process by selenium abstraction in 131.67

**Scheme 30** Cascade radical reactions of vinyl radicals involving 1,6-HAT at  $C(sp^3)$ —H sites  $\alpha$ - to heteroatom.

# **HAT** involving aryl radicals

Aryl radicals are extremely reactive species. Similarly with HAT to vinyl radicals, HAT to aryl radicals from aliphatic C–H sites is energetically favourable due to high BDE difference of aryl C–H bonds (Ph–H, BDE = 112 kcal/mol) compared to that of aliphatic C–H bonds (BDE ~96–100 kcal/mol).<sup>47</sup> In 1954, Hey and coworkers recognized intramolecular 1,5-HAT during the decomposition of *o*-(dimethylaminocarbonyl)aryl or (*N*-aryl-*N*-methylaminocarbonyl)aryl diazonium salts.<sup>8</sup> Later, Cohen and co-workers also showed that aryl radicals could undergo 1,5-HAT during copper-catalyzed decomposition of diazonium salts, which was supported by extensive mechanistic studies.<sup>68</sup> The deuterium labelling experiments suggested that rate of 1,5-HAT is much faster than the rotation around amide C–N bond but slower than that of methyl C(sp³)–N bond, presumably due to

partial double bond character of the former. In 1978, Pines and co-workers reported intramolecular HAT process of aryl radicals generated from different ortho-substituted aryl diazonium salts. Furthermore, intramolecular 1,5-, 1,6-, 1,7-HAT were observed during copper-catalyzed decomposition of *o*-di-*n*-propylaminosulfonylbenzenediazonium salts.<sup>69</sup>

#### Intramolecular HAT

#### 1,5-HAT

In their pioneering works, Curran group reported translocation of radicals from C(sp<sup>2</sup>) to C(sp<sup>3</sup>)-H sites via 1,5-HAT.<sup>9a,70</sup> Incorporated into a modified 'protecting group' of alcohols, aryl radical serves as an HAT agent to produce translocated alkyl radical (Scheme 31). The latter is trapped intramolecularly followed by reduction by tin hydride to deliver cyclopentane derivatives 137-140. A premature reduction of radicals A or B via intermolecular HAT from Bu<sub>3</sub>SnH could produce acyclic alkene byproducts 135-136. As shown in their first report in 1988, introduction of silicon-based tether led to improvement of product to side reduction byproduct ratio (137c vs 135c). Few years later, the same group introduced o-bromo-pmethoxyphenyl ethers as a new radical translocating groups for  $\beta$  C–H bond activation (138a–c). The deuterium labelling study showed that tertiary radicals were efficiently generated, however translocation of radical to the secondary C-H sites were challenging due to a competitive 1,6-HAT process. Introduction of ortho substituents (138c) improved the efficiency of radical translocation process. Of note, in the absence of double bond tether, extrusion of stable benzylic radical occurs, leading to the corresponding aldehyde or ketone.71

Similarly, amides have also been utilized in the related process involving 1,5-HAT step. 72 In the case of o-iodobenzamides, 72a, b only the anti-rotamer of **134f** will lead to the desired cyclic product (**139a–c**). Thus, the reaction outcome is highly dependent on the R group as it affects the anti/syn ratio of the amide. On the other hand, employment of o-iodoanilides allows for the direct  $\alpha$  C–H functionalization of carbonyl compounds without enol or enolate formation. 72c, d The reaction is shown to be effective for intermolecular radical trapping of the translocated radical with deuterium or allylic group (**140d**).

**Scheme 31** Translocation of radicals from  $C(sp^2)$ - to  $C(sp^3)$  sites via 1,5-HAT, followed by cyclization to afford cyclopentane derivatives.

In 2016, Gevorgyan group introduced a 1,5-HAT event of hybrid palladium-radical species (Scheme 32). Aryl halides are well-known substrates in palladium catalysis, typically involved in two-electron oxidative addition process. Whereas, in this case the authors have uncovered that irradiation of blue light switched the reaction pathway leading to an SET process to generate hybrid palladium-radical species **A**. Due to the radical nature of this intermediate, it undergoes 1,5-HAT process to generate translocated radical species **B**, which upon  $\beta$ -hydrogen loss delivers silyl enol ethers **142a–d**. In this light-induced protocol, palladium plays a double duty by harvesting light and catalyzing bond breaking/forming process. Notably, this mild method for dehydrogenation of silyl-protected alcohols to silyl enol ethers proceeds at room temperature without use of exogeneous photosensitisers or oxidants.

Scheme 32 HAT event of hybrid Pd-radical species.

In 1994, Weinreb group utilized copper catalyzed diazotation of o-aminobenzamides 143 for oxidation of amides, which can also be translated to more complex systems like 144d, used in synthesis of antibiotic anisomycin (Scheme 33).74 In this case, in situ diazotization of o-aminobenzamide 143, followed by reduction via SET from copper catalyst generates aryl radical A. 1,5-HAT of the latter affords nucleophilic radical **B**, which then via the copper-catalyzed radical-polar crossover process gets oxidized into  $\alpha$ -amino carbocation that is trapped by methanol to deliver products 144a-d. Recently, Qi and Zhang group reported photocatalytic, metal-free methods with similar type of substrates to achieve  $\alpha$ -amino C(sp³)–H functionalization.<sup>75</sup> Likewise, single electron reduction of the in situ formed diazonium salt by excited Eosin Y photocatalyst leads to aryl intermediate, which eventually affords alkoxybenzamides (145a-d) in moderate to good yields.

Scheme 33 Oxidation of amides via 1,5-HAT.

At the same time, Zeng and co-workers reported site-selective silylation of  $\alpha$ -amino C(sp³)–H bond (Scheme 34).<sup>76</sup> The use of Grignard reagent enables generation of *N*-magnesiated aryl radical **A** from the corresponding fluoride **146**. This method represents the first example of  $\alpha$  C–H silylation of amides.

Scheme 34 Silylation of benzamides via 1,5-HAT.

It has been shown that in the absence of tethered alkene as in the previous examples (Scheme 31), the translocated radical B can undergo radical addition to arene, thus affording cyclization products 149-152 after rearomatization (Scheme 35). In 2013, Kalyani and co-workers reported the use of nickel or phenanthroline catalyst for aryl chlorides and bromides to afford various isoindolin-1-ones **149a–d**.<sup>77</sup> Shortly after, Kumar group developed metal-free conditions targeting bromides and iodides to deliver similar products (150a-d).78 In 2016, Xu group employed iridium photocatalysis to achieve similar transformations (148 -> 151) with iodides and its applications to the formal syntheses of (±)-coerulescine and (±)physovenine.<sup>79</sup> More recently, Gevorgyan and co-workers achieved the first photoinduced palladium-catalyzed C(sp²)-O bond activation of aryl triflate to form hybrid aryl palladiumradical intermediate,80 which underwent the same sequence of 1,5-HAT/radical cyclization to afford oxyindole and isoindolin-1ones 152a-d.

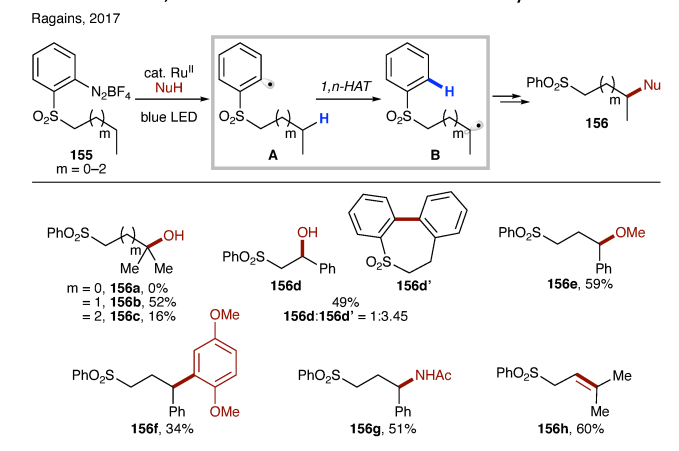
**Scheme 35** Synthesis of fused systems via 1,5-HAT from C(sp³)– H to C(sp²) site followed by radical cyclization at aromatic ring.

#### 1,6-HAT

In 2016, Fu and co-workers reported transition metal-free, intramolecular, regioselective cross dehydrogenative coupling of aliphatic and aromatic C–H bonds (Scheme 36). The authors used readily available aryl triazine **153** and cheap oxidant,  $K_2S_2O_8$ , to generate under thermal conditions aryl radical **A**. The latter undergoes selective 1,6-HAT at the aliphatic C–H sites to afford translocated  $\beta$ -amino alkyl radical **B**, which cyclizes to from six membered cyclic anilides **154a–d**. Notably, phenyl alanine-derived substrates exhibit very high diastereoselectivity, leading to cis isomers (**154c**). In contrast, reactions of substrate containing aspartic acid derivatives led to statistical mixture of diastereomers (**154d**).

**Scheme 36** Synthesis of cyclic anilides involving 1,6-HAT from the aliphatic C–H sites.

Recently, Ragains group developed photocatalytic reduction of ortho-diazoniaphenyl alkyl sulfones for remote  $C(sp^3)$ –H functionalization (Scheme 37). First photoexcited Ru-catalyst undergoes SET to diazonium salts **155**, followed by nitrogen loss leading to aryl radical **A**. This electrophilic aryl radical then undergoes intramolecular HAT at alkyl or benzylic C–H sites, preferably in 1,6-fashion ( $A \rightarrow B$ ). The formed nucleophilic radical undergoes radical polar cross over via single electron oxidation by the photocatalyst or by the substrate via chain process into a carbocation. A subsequent trapping of the latter with different nucleophiles afford remote hydroxylation (**156a**–**d**), etherification (**156e**), C–C bond formation (**156f**), amidation (**156g**), as well as desaturation (**156h**) products. In this protocol, the possibility of 1,5-HAT, as well as 1,7-HAT, was demonstrated, albeit with much lower efficiency.



**Scheme 37** 1,6-HAT to aryl ring of aryl sulfones from aliphatic  $C(sp^3)$ -H sites.

## 1,7-HAT

In 2012, Baran group established a dehydrogenation method for guided desaturation of unactivated C(sp³)–H sites of alcohols and amines (Scheme 38a).<sup>83</sup> Under acidic conditions,

aryl triazene **157** is in situ converted into diazonium salt, which upon reductive decomposition leads to aryl radical **A**. The latter is capable of undergoing intramolecular HAT to form nucleophilic alkyl radical **B**, which is further oxidized to the corresponding carbocation via a radical polar crossover scenario ( $\mathbf{B} \rightarrow \mathbf{C}$ ) by TEMPO+ formed at the early stages of the reaction. Loss of proton affords remote desaturation products **158a**–**e**. For this sulfonyl tether, **1**,7-HAT is more preferable, however, presence of weaker  $\beta$ C–H bonds could lead to **1**,6-HAT products (**158b**). It is also shown that even **1**,8-HAT is possible at activated allylic C–H site of **157e** to deliver diene **158e**.

In 2015, Regains and co-workers uncovered remote hydroxylation of alcohols and amines with similar type of aryl sulfonyl tethers under photocatalytic conditions (Scheme 38b).<sup>84</sup> In this protocol, instead of TEMPO, a photocatalyst enables the single-electron redox process to afford after solvolysis the hydroxylation products **160a–d**. Expectedly, as in the above case, the aryl sulfonyl tether favours 1,7-HAT, unless a weaker benzylic C–H site is present to promote 1,6-HAT event.

**Scheme 38** (a) Guided desaturation of aliphatic alcohols and amines via intramolecular HAT. (b) Remote hydroxylation via intramolecular HAT.

In 2018, Gevorgyan group developed mild photo-induced palladium-catalyzed protocol for proximal and remote desaturation of aliphatic amines (Scheme 39).85 This method utilizes readily available 2-iodocarbonyl or 2-iodosulfonyl tethers (162) which could be routinely installed and do not require isolation. Under the reaction conditions, photoexcited palladium undergoes single electron transfer to aryl iodide to form electrophilic aryl radical  $\mathbf{A}$ , which undergoes 1,n-HAT (n = 5–7) (**A**  $\rightarrow$  **B**) to afford translocated alkyl radical at  $\alpha$ -,  $\beta$ -, or  $\gamma$ -C(sp³)-H sites of amines depending upon the type of tether used. The translocated palladium hybrid radical undergoes regioselective  $\beta$ -H loss to afford desaturation product, either via radical recombination, followed by  $\beta$ -hydride elimination or via direct H-abstraction by Pd(I) species. In this report, the authors utilized carbonyl tether for 1,5-HAT (163a), whereas aryl sulfonyl tether for 1,7- (163c-d), as well as 1,6-HAT (163b and 163b')

**Scheme 39** Remote desaturation of aliphatic amines via HAT from C(sp³)—H site.

In the same year, Studer group reported translocation of aryl radicals from sulfonyl group to alkyl C–H sites (Scheme 40).<sup>86</sup> In this protocol, they have used thermal conditions and AIBN for radical initiation, which abstracts weak hydrogen of tris(trimethylsillyl)silane to generate super silyl radical, which abstracts iodine atom from the substrate **164** to generate aryl radical **A**, which undergoes 1,7-HAT at unactivated C(sp³)–H sites of alcohols to produce **B**. The translocated nucleophilic radical undergoes radical Smiles-type rearrangement to afford remote arylated products **165a–c**.

**Scheme 40** Arylation of alcohols via 1,7-HAT, followed by aryl group migration.

### Intermolecular HAT

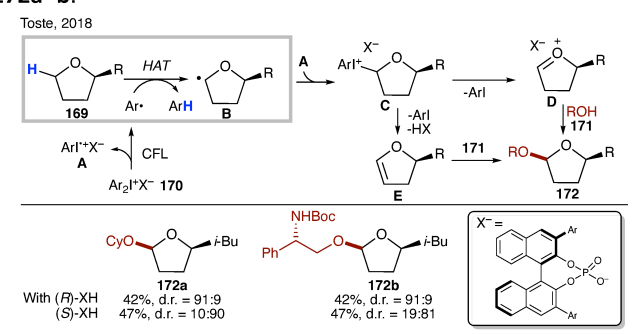
In contrast to *O*-centered radicals,  $^{7c,87}$  *C*-centered radicals are less efficient for intermolecular HAT. Thus, examples of intermolecular HAT by aryl radical at  $C(sp^3)$ —H sites are scarce in literature, mostly limited to activated C—H bonds or use of C—H source as a solvent. HAT from tetrahydrofuran or toluene by phenyl radical is very fast process, rates are  $4.8\times10^6$  M $^{-1}s^{-1}$  and  $1.7\times10^6$  M $^{-1}s^{-1}$ , respectively.  $^{88}$  Due to high reactivity of aryl radicals, other side reactions, including addition to arene and alkene or halogen abstraction reactions are also capable processes.

In 2005, Porta and co-workers reported systematic study of intermolecular HAT by aryl radical at C–H sites of tetrahydrofuran and other ethers (Scheme 41).<sup>89</sup> They have demonstrated that under aqueous conditions, phenyl radicals, generated from single electron reduction of diazonium salt, are able to intermolecularly abstract hydrogen atom to form nucleophilic  $\alpha$ -alkoxy radicals **A**. The latter adds to the in situ formed iminium salt **B** to afford after reduction by Ti(III) species 1,2-aminoalcohol derivatives **168a–c**.

Scheme 41 Aminoalkylation of ethers via intermolecular HAT.

Recently, Toste group reported an interesting light-induced chiral diaryliodonium phosphate-mediated diastereoselective  $\alpha$ -acetalization of cyclic ethers (Scheme 42). 90 Photochemically active diaryliodonium salt **170** is homolyzed under light irradiation to generate aryl radical and aryl iodonium radical cation **A**, the former undergoes a regioselective intermolecular

HAT with substrate **169** to produce  $\alpha$ -alkoxy radical **B**, which then recombines with **A** to give iodonium species **C**. A subsequent elimination leads to intermediate **D** or **E**, which upon chiral diaryliodonium phosphate salt-assisted nucleophilic attack of alcohol **171** delivers the enantioenriched products **172a**-b.



**Scheme 42** Chiral diaryliodonium phosphate-mediated diastereoselective  $\alpha$ -acetalization of cyclic ethers involving intermolecular HAT.

More recently, Li, Zhang, Yang, Walsh and co-workers developed transition metal-free dehydrogenative cross-coupling of *N*-benzyl amines and saturated heterocycles (Scheme 43).<sup>91</sup> They have shown that 2-azaallyl anion **A**, generated by deprotonation of *N*-benzyl amines, can undergo SET to aryl iodide to form aryl radical and persistent 2-azaallyl radical **B**. Sterically protected sacrificial aryl radical undergoes intermolecular HAT at activated C(sp³)—H sites to form stabilized nucleophilic radical **C**, which recombines with persistent 2-azaallylradical **B** to deliver the products **174a**–**d**.

**Scheme 43** Dehydrogenative cross-coupling via intermolecular HAT.

# **Conclusions**

Organic radical chemistry enjoyed a prosperous period back in the 90's, which resulted in ground-breaking developments of C—H functionalization via HAT pathway. Recent discoveries of mild methods for generation of radicals, which obviate the use of conventional radical initiators (e.g. AIBN, Et<sub>3</sub>B) and reagents (e.g. Bu<sub>3</sub>SnH, (TMS)<sub>3</sub>SiH), led to a renaissance of the field, as manifested by the booming literature examples. C—H functionalization via HAT often distinguishes itself from

transition metal-based two-electron approaches in respect of site selectivity. This complementary feature has opened up numerous opportunities to tackle longstanding problems in organic synthesis, as partially exemplified by the recent advances summarized in this Review. With that being said, HAT mediated by C-centered radical, as compared to the N- and Ocentered analogues, is still underdeveloped and mostly confined to intramolecular activation. Thus, a deeper understanding of the nature and guiding parameters of reactivity is needed to harness full potential of C-centered radical in more challenging and complex settings, which may in turn lead to the design of novel C-centered radical precursors. Furthermore, enantioselective HAT via N-centered radicals has been achieved very recently,92 thus providing the basis and motivation for development of enantioselective HAT processes. It is foreseeable that an asymmetric variant of C-centered radical-mediated HAT will mark a major breakthrough in this area. Undoubtedly, the progress of C-centered radical chemistry will further the field of C-H functionalization in near future.

#### Conflicts of interest

The authors declare no conflict of interest.

# **Acknowledgements**

We thank the National Institute of Health (GM120281), National Science Foundation (CHE-1955663), and Welch Foundation (Chair, AT-0041) for financial support.

## **Notes and references**

- 1. (a) J. Yamaguchi, A. D. Yamaguchi and K. Itami, *Angew. Chem., Int. Ed.*, 2012, **51**, 8960-9009; (b) J. Wencel-Delord and F. Glorius, *Nat. Chem.*, 2013, **5**, 369-375; (c) D. Y. K. Chen and S. W. Youn, *Chem. Eur. J.*, 2012, **18**, 9452-9474; (d) T. Cernak, K. D. Dykstra, S. Tyagarajan, P. Vachal and S. W. Krska, *Chem. Soc. Rev.*, 2016, **45**, 546-576.
- 2. (a) R. G. Bergman, *Nature*, 2007, **446**, 391-393; (b) M. C. White, *Science*, 2012, **335**, 807-809.
- 3. (a) H. M. Davies and J. R. Manning, *Nature*, 2008, **451**, 417-424; (b) R. Giri, B. F. Shi, K. M. Engle, N. Maugel and J. Q. Yu, *Chem. Soc. Rev.*, 2009, **38**, 3242-3272; (c) T. W. Lyons and M. S. Sanford, *Chem. Rev.*, 2010, **110**, 1147-1169; (d) I. A. Mkhalid, J. H. Barnard, T. B. Marder, J. M. Murphy and J. F. Hartwig, *Chem. Rev.*, 2010, **110**, 890-931; (e) J. L. Roizen, M. E. Harvey and J. Du Bois, *Acc. Chem. Res.*, 2012, **45**, 911-922; (f) F. Kakiuchi and N. Chatani, *Adv. Synth. Catal.*, 2003, **345**, 1077-1101.
- 4. (a) J. M. Mayer, *Acc. Chem. Res.*, 2011, **44**, 36-46; (b) M. Salamone and M Bietti, *Acc. Chem. Res.*, 2015, **48**, 2895-2903; (c) S. A. Green, S. W. M. Crossley, J. L. M. Matos, S. Vásquez-Céspedes, S. L. Shevick and R. A. Shenvi, *Acc. Chem. Res.*, 2018, **51**, 2628-2640; (d) M. Milan, M. Salamone, M. Costas and M. Bietti, *Acc. Chem. Res.*, 2018, **51**, 1984-1995.
- 5. J. C. K. Chu and T. Rovis, *Angew. Chem.*, *Int. Ed.*, 2018, **57**, 62-101.

- 6. (a) A. W. Hofmann, *Chem. Ber.*, 1883, **16**, 558-560; (b) K. Löffler and C. Freytag, *Chem. Ber.*, 1909, **42**, 3427-3431; (c) D. H. R. Barton, J. M. Beaton, L. E. Geller and M. M. Pechet, *J. Am. Chem. Soc.*, 1961, **83**, 4076-4083.
- 7. (a) J. Robertson, J. Pillai and R. K. Lush, *Chem. Soc. Rev.*, 2001, **30**, 94-103; (b) M. Nechab, S. Mondal and M. P. Bertrand, *Chem. Eur. J.*, 2014, **20**, 16034-16059; (c) L. Capaldo and D. Ravelli, *Eur. J. Org. Chem.*, 2017, **2017**, 2056-2071; (d) L. M. Stateman, K. M. Nakafuku and D. A. Nagib, *Synthesis*, 2018, **50**, 1569-1586; (e) H. Chen and S. Yu, *Org. Biomol. Chem.*, 2020, **18**, 4519-4532; (f) N. Goswami and D. Maiti, *Isr. J. Chem.*, 2020, **60**, 303-312; (g) G. Kumar, S. Pradhan and I. Chatterjee, *Chem. Asian J.*, 2020, **15**, 651-672.
- 8. D. H. Hey and D. G. Turpin, J. Chem. Soc., 1954, 2471-2481.
- 9. (a) D. P. Curran, D. Kim, H. T. Liu and W. Shen, *J. Am. Chem. Soc.*, 1988, **110**, 5900-5902; (b) D. C. Lathbury, P. J. Parsons and I. Pinto, *J. Chem. Soc.*, *Chem. Comm.*, 1988, 81-82.
- 10. (a) M. D. E. Forbes, J. T. Patton, T. L. Myers, H. D. Maynard, D. W. Smith, G. R. Schulz and K. B. Wagener, *J. Am. Chem. Soc.*, 1992, **114**, 10978-10980; (b) C. Toniolo, M. Crisma, F. Formaggio and C. Peggion, *Biopolymers* 2001, **60**, 396-419.
- 11. M. C. White and J. Zhao, *J. Am. Chem. Soc.*, 2018, **140**, 13988-14009.
- 12. W. Shu and C. Nevado, *Angew. Chem., Ind. Ed.*, 2017, **56**, 1881-1884.
- 13. (a) K. Héberger and A. Lopata, *J. Org. Chem.*, 1998, **63**, 8646-8653; (b) F. De Vleeschouwer, V. Van Speybroeck, M. Waroquier, P. Geerlings and F. De Proft, *Org. Lett.*, 2007, **9**, 2721-2724; (c) L. Jing, J. J. Nash and H. I. Kenttämaa, *J. Am. Chem. Soc.*, 2008, **130**, 17697-17709; (d) F. D. Vleeschouwer, V. V. Speybroeck, Michel Waroquier, P. Geerlings and F. D. Proft, *J. Org. Chem.*, 2008, **73**, 9109-9120; (e) F. De Vleeschouwer, P. Geerlings and F. De Proft, *Theor. Chem. Acc.*, 2012, **131**, 1245; (f) L. R. Doming and P. Pérez, Org. Biomol. Chem., 2013, **11**, 4350-4358.
- 14. (a) J. E. Bennett, B. C. Gilbert, S. Lawrence, A. C. Whitwood and A. J. Holmes, *J. Chem. Soc., Perkin Trans. 2*, 1996, **2**, 1789-1795; (b) D. Ravelli, M. Fagnoni, T. Fukuyama, T. Nishikawa and I. Ryu, *ACS Catal.*, 2018, **8**, 701-713.
- 15. (a) S. J. Cole, J. N. Kirwan, B. P. Roberts and C. R. Willis, *J. Chem. Soc., Perkin Trans.* 1, 1991, 103-112; (b) B. P. Roberts *Chem. Soc. Rev.*, 1999, **28**, 25-35; (c) B. Chan, C. J. Easton and L. Radom, *J. Phys. Chem. A*, 2015, **119**, 3843-3847.
- 16. (a) X. L. Huang and J. J. Dannenberg, *J. Org. Chem.*, 1991, **56**, 5421-5424; (b) Y. Chen and E. Tschuikow-Roux, *J. Phys. Chem.*, 1993, **97**, 3742-3749.
- 17. D. Kurandina, D. Yadagiri, M. Rivas, A. Kavun, P. Chuentragool, K. Hayama and V. Gevorgyan, *J. Am. Chem. Soc.*, 2019, **141**, 8104-8109. 18. (a) D. J. Hart and S. C. Wu, *Tetrahedron Lett.*, 1991, **32**, 4099-4102; (b) S. Atarashi, J. K. Choi, D. C. Ha, D. J. Hart, D. Kuzmich, C. S. Lee, S. Ramesh and S. C. Wu, *J. Am. Chem. Soc.*, 1997, **119**, 6226-6241.
- 19. (a) J. Brunckova, D. Crich and Q. W. Yao, *Tetrahedron Lett.*, 1994, **35**, 6619-6622; (b) D. Crich, S. Sun and J. Brunckova, *J. Org. Chem.*, 1996, **61**, 605-615.
- 20. J. Cassayre and S. Z. Zard, *J. Organomet. Chem.*, 2001, **624**, 316-
- 21. M. Nechab, S. Mondal and M. P. Bertrand, *Chem. Eur. J.*, 2014, **20**, 16034-16059.
- 22. (a) M. Tojino, Y. Uenoyama, T. Fukuyama and I. Ryu, *Chem. Commun.*, 2004, 2482-2483; (b) I. Ryu, T. Fukuyama, M. Tojino, Y. Uenoyama, Y. Yonamine, N. Terasoma and H. Matsubara, *Org. Biomol. Chem.*, 2011, **9**, 3780-3786.

- 23. M. S. Wilson, J. C. Woo and G. R. Dake, *J. Org. Chem.*, 2006, **71**, 4237-4245.
- 24. G. R. Dake, E. E. Fenster and B. O. Patrick, *J. Org. Chem.*, 2008, **73**, 6711-6715.
- 25. W. Yuan, Y. Wei, M. Shi and Y. Li, *Chem. Eur. J.*, 2012, **18**, 1280-1285.
- 26. F. Scully and H. Morrison, *J. Chem. Soc., Chem. Comm.*, 1973, 529-530
- 27. A. C. Pratt, J. Chem. Soc., Chem. Comm., 1974, 183-184.
- 28. (a) J. M. Hornback, L. G. Mawhorter, S. E. Carlson and R. A. Bedont, *J. Org. Chem.*, 1979, **44**, 3698-3703; (b) J. M. Hornback and R. D. Barrows, *J. Org. Chem.*, 1982, **47**, 4285-4291.
- 29. T. Peez, V. Schmalz, K. Harms and U. Koert, *Org. Lett.*, 2019, **21**, 4365-4369.
- 30. (a) P. Yu, J. S. Lin, L. Li, S. C. Zheng, Y. P. Xiong, L. J. Zhao, B. Tan and X. Y. Liu, *Angew. Chem., Int. Ed.*, 2014, **53**, 11890-11894; (b) P. Yu, S. C. Zheng, N. Y. Yang, B. Tan and X. Y. Liu, *Angew. Chem., Int. Ed.*, 2015, **54**, 4041-4045.
- 31. (a) G. H. Lonca, D. Y. Ong, T. M. H. Tran, C. Tejo, S. Chiba and F. Gagosz, *Angew. Chem., Int. Ed.,* 2017, **56**, 11440-11444; (b) H. Hayashi, A. Kaga, B. Wang, F. Gagosz and S. Chiba, *Chem. Commun.*, 2018, **54**, 7535-7538; (c) W. Shu, E. Merino and C. Nevado, *ACS Catal.*, 2018, **8**, 6401-6406; (d) L. Li, H. Luo, Z. Zhao, Y. Li, Q. Zhou, J. Xu, J. Li and Y. N. Ma, *Org. Lett.*, 2019, **21**, 9228-9231.
- 32. (a) L. Huang, S. C. Zheng, B. Tan and X. Y. Liu, *Chem. Eur. J.*, 2015, **21**, 6718-6722; (b) L. Huang, J. S. Lin, B. Tan and X. Y. Liu, *ACS Catal.*, 2015, **5**, 2826-2831.
- 33. (a) L. Li, L. Ye, S. F. Ni, Z. L. Li, S. Chen, Y. M. Du, X. H. Li, L. Dang and X. Y. Liu, *Org. Chem. Front.*, 2017, **4**, 2139-2146; (b) N. Wang, L. Ye, Z. L. Li, L. Li, Z. Li, H. X. Zhang, Z. Guo, Q. S. Gu and X. Y. Liu, *Org. Chem. Front.*, 2018, **5**, 2810-2814; (c) J. Zhang, W. Jin, C. Cheng and F. Luo, *Org. Biomol. Chem.*, 2018, **16**, 3876-3880. (d) E. P. Farney, S. S. Feng, F. Schäfers and S. E. Reisman, *J. Am. Chem. Soc.*, 2018, **140**, 1267-1270.
- 34. (a) W. Jin, Y. Zhou, Y. Zhao, Q. Ma, L. Kong and G. Zhu, *Org. Lett.*, 2018, **20**, 1435-1438; (b) J. H. Yang, X. B. Fu, Z. H. Lu and G. G. Zhu, *Acta Chim. Sinica*, 2019, **77**, 901-905.
- 35. K. J. Bian, Y. Li, K. F. Zhang, Y. He, T. R. Wu, C. Y. Wang and X. S. Wang, *Chem. Sci.*, 2020, **11**, 10437-10443.
- 36. P. C. Van Dort and P. L. Fuchs, *J. Org. Chem.*, 1997, **62**, 7142-7147. 37. A. Attouche, D. Urban and J. M. Beau, *Angew. Chem., Int. Ed.*, 2013, **52**, 9572-9575.
- 38. X. Xiao, Z. Xu, Q. D. Zeng, X. B. Chen, W. H. Ji, Y. Han, P. Wu, J. Ren and B. B. Zeng, *Chem. Eur. J.*, 2015, **21**, 8351-8354.
- 39. M. Parasram, P. Chuentragool, Y. Wang, Y. Shi and V. Gevorgyan, *J. Am. Chem. Soc.*, 2017, **139**, 14857-14860.
- 40. For examples on unusual *endo-trig* radical cyclizations of silyltethered radicals due to longer Si-C and Si-O bonds, see: (a) M. Koreeda and L. G. Hamann, *J. Am. Chem. Soc.*, 1990, **112**, 8175-8177; (b) M. Parasram, V. O. laroshenko and V. Gevorgyan, *J. Am. Chem. Soc.*, 2014, **136**, 17926-17929.
- 41. For selected reviews, see: (a) D. Kurandina, P. Chuentragool and V. Gevorgyan, *Synthesis*, 2019, **51**, 985-1005; (b) P. Chuentragool, D. Kurandina and V. Gevorgyan, *Angew. Chem., Int. Ed.*, 2019, **58**, 11586-11598; (c) R. Kancherla, K. Muralirajan, A. Sagadevan and M. Rueping, *Trends Chem.*, 2019, **1**, 510-523; (d) W.-J. Zhou, G.-M. Cao, Z.-P. Zhang and D.-G. Yu, *Chem. Lett.*, 2019, **48**, 181-191; (e) W. M. Cheng and R. Shang, *ACS Catal.*, 2020, **10**, 9170-9196. For selected examples of alkyl Heck reaction, see: (f) D. Kurandina, M. Parasram and V. Gevorgyan, *Angew. Chem., Int. Ed.*, 2017, **56**, 14212-14216; (g) G. Z. Wang, R. Shang, W. M. Cheng and Y. Fu, *J. Am. Chem. Soc.*, 2017, **139**, 18307-18312; (h) D. Kurandina, M. Rivas, M. Radzhabov

- and V. Gevorgyan, *Org. Lett.*, 2018, **20**, 357-360; (i) M. Koy, F. Sandfort, A. Tlahuext-Aca, L. Quach, C. G. Daniliuc and F. Glorius, *Chem. Eur. J.*, 2018, **24**, 4552-4555; (j) R. Kancherla, K. Muralirajan, B. Maity, C. Zhu, P. E. Krach, L. Cavallo and M. Rueping, *Angew. Chem., Int. Ed.*, 2019, **58**, 3412-3416.
- 42. P. Chuentragool, D. Yadagiri, T. Morita, S. Sarkar, M. Parasram, Y. Wang and V. Gevorgyan, *Angew. Chem., Int. Ed.*, 2019, **58**, 1794-1798
- 43. K. Yamada, H. Fujihara, Y. Yamamoto, Y. Miwa, T. Taga and K. Tomioka, *Ora. Lett.*, 2002, **4**, 3509-3511.
- 44. K. Yamada, Y. Yamamoto and K. Tomioka, *Org. Lett.*, 2003, **5**, 1797-1799.
- 45. (a) P. Lu, T. Hou, X. Gu and P. Li, *Org. Lett.*, 2015, **17**, 1954-1957; (b) T. Hou, P. Lu and P. Li, *Tetrahedron Lett.*, 2016, **57**, 2273-2276; (c) Y. Otake, J. D. Williams, J. A. Rincon, O. de Frutos, C. Mateos and C. O. Kappe, *Org. Biomol. Chem.*, 2019, **17**, 1384-1388.
- 46. C. J. Wallentin, J. D. Nguyen, P. Finkbeiner and C. R. J. Stephenson, *J. Am. Chem. Soc.*, 2012, **134**, 8875-8884.
- 47. Y.-R. Luo, *Comprehensive Handbook of Chemical Bond Energies*, CRC Press, 2007; (b) S. J. Blanksby and G. B. Ellison, *Acc. Chem. Res.* 2003, **36**, 255-263.
- 48. B. C. Gilbert and D. J. Parry, *J. Chem. Soc., Perkin Trans. 2*, 1988, 875-886.
- 49. F. Dénès, F. Beaufils and P. Renaud, Synlett, 2008, 2389-2399.
- (a) U. Wille, Chem. Rev., 2013, 113, 813-853; (b) E. I. Heiba and R.
   M. Dessau, J. Am. Chem. Soc., 1967, 89, 3772-3777.
- 51. M. Gulea, J. M. Lopez-Romero, L. Fensterbank and M. Malacria, *Org. Lett.*, 2000, **2**, 2591-2594.
- 52. M. M. Logan, T. Toma, R. Thomas-Tran and J. Du Bois, *Science*, 2016, **354**, 865-869.
- 53. D. P. Curran and W. Shen, *J. Am. Chem. Soc.*, 1993, **115**, 6051-6059.
- 54. M. Ratushnyy, M. Parasram, Y. Wang and V. Gevorgyan, *Angew. Chem.*, *Int. Ed.*, 2018, **57**, 2712-2715.
- 55. E.-A. I. Heiba and R. M. Dessau, *J. Am. Chem. Soc.*, 1967, **89**, 3772-3777.
- 56. E. Bosch and M. D. Bachi, J. Org. Chem., 1993, 58, 5581-5582.
- 57. S. Bogen, M. Gulea, L. Fensterbank and M. Malacria, *J. Org. Chem.*, 1999, **64**, 4920-4925.
- 58. R. Bénéteau, C. F. Despiau, J. C. Rouaud, A. Boussonnière, V. Silvestre, J. Lebreton and F. Dénès, *Chem. Eur. J.*, 2015, **21**, 11378-11386.
- 59. (a) S. Wu, X. Wu, D. Wang and C. Zhu, *Angew. Chem., Int. Ed.*, 2019, **58**, 1499-1503; (b) S. Yang, X. Wu, S. Wu and C. Zhu, *Org. Lett.*, 2019, **21**, 4837-4841.
- 60. (a) T. Shang, J. Zhang, Y. Zhang, F. Zhang, X. S. Li and G. Zhu, *Org. Lett.*, 2020, **22**, 3667-3672; (b) Z. Xiong, F. Zhang, Y. Yu, Z. Tan and G. Zhu, *Org. Lett.*, 2020, **22**, 4088-4092.
- 61. H. Li, L. Guo, X. L. Feng, L. P. Huo, S. Q. Zhu and L. L. Chu, *Chem. Sci.*, 2020, **11**, 4904-4910.
- 62. P. Devin, L. Fensterbank and M. Malacria, *J. Org. Chem.*, 1998, **63**, 6764-6765.
- 63. G. M. Allan, A. F. Parsons and J. F. Pons, *Synlett*, 2002, 1431-1434.64. H. Lin, A. Schall and O. Reiser, *Synlett*, 2005, 2603-2606.
- 65. S. K. Pagire and O. Reiser, Green Chem., 2017, 19, 1721-1725.
- 66. (a) J. K. Vellucci and C. M. Beaudry, *Org. Lett.*, 2015, **17**, 4558-4560; (b) R. Kim, A. J. Ferreira and C. M. Beaudry, *Angew. Chem., Int. Ed.*, 2019, **58**, 12595-12598.
- 67. Y. Yoshimura, Y. Yamazaki, K. Wachi, S. Satoh and H. Takahata, Synlett, 2007, 111-114.

- 68. (a) A. H. Lewin, A. H. Dinwoodie and T. Cohen, *Tetrahedron*, 1966, **22**, 1527-1537; (b) T. Cohen, C. H. McMullen and K. Smith, *J. Am. Chem. Soc.*, 1968, **90**, 6866-6867.
- 69. S. H. Pines, R. M. Purick, R. A. Reamer and G. Gal, *J. Org. Chem.*, 1978, **43**, 1337-1342.
- 70. D. P. Curran and J. Xu, *J. Am. Chem. Soc.*, 1996, **118**, 3142-3147.
- 71. D. P. Curran and H. S. Yu, Synthesis, 1992, 123-127.
- 72. (a) V. Snieckus, J. C. Cuevas, C. P. Sloan, H. T. Liu and D. P. Curran, *J. Am. Chem. Soc.*, 1990, **112**, 896-898; (b) D. P. Curran and H. T. Liu, *J. Chem. Soc.*, *Perkin Trans.* 1, 1994, 1377-1393; (c) D. P. Curran, A. C. Abraham and H. T. Liu, *J. Org. Chem.*, 1991, **56**, 4335-4337; (d) D. P. Curran, H. S. Yu and H. T. Liu, *Tetrahedron*, 1994, **50**, 7343-7366.
- 73. M. Parasram, P. Chuentragool, D. Sarkar and V. Gevorgyan, *J. Am. Chem. Soc.*, 2016, **138**, 6340-6343.
- 74. G. H. Han, M. C. Mcintosh and S. M. Weinreb, *Tetrahedron Lett.*, 1994, **35**, 5813-5816.
- 75. F.-Q. Huang, X. Dong, L.-W. Qi and B. Zhang, *Tetrahedron Lett.*, 2016, **57**, 1600-1604.
- 76. P. Liu, J. Tang and X. Zeng, Org. Lett., 2016, 18, 5536-5539.
- 77. (a) W. C. Wertjes, L. C. Wolfe, P. J. Waller and D. Kalyani, *Org. Lett.*, 2013, **15**, 5986-5989; (b) W. C. Wertjes, P. J. Waller, K. E. Shelton and D. Kalyani, *Synthesis*, 2014, **46**, 3033-3040.
- 78. B. S. Bhakuni, A. Yadav, S. Kumar, S. Patel, S. Sharma and S. Kumar, *J. Org. Chem.*, 2014, **79**, 2944-2954.
- 79. J. Q. Chen, Y. L. Wei, G. Q. Xu, Y. M. Liang and P. F. Xu, *Chem. Commun.*, 2016, **52**, 6455-6458.
- 80. M. Ratushnyy, N. Kvasovs, S. Sarkar and V. Gevorgyan, *Angew. Chem., Int. Ed.*, 2020, **59**, 10316-10320.
- 81. H. Tian, H. Yang, C. Zhu and H. Fu, Sci. Rep., 2016, 6, 19931.
- 82. S. Du, E. A. Kimball and J. R. Ragains, *Org. Lett.*, 2017, **19**, 5553-5556.
- 83. A. F. Voica, A. Mendoza, W. R. Gutekunst, J. O. Fraga and P. S. Baran, *Nat. Chem.*, 2012, **4**, 629-635.
- 84. K. A. Hollister, E. S. Conner, M. L. Spell, K. Deveaux, L. Maneval, M. W. Beal and J. R. Ragains, *Angew. Chem., Int. Ed.*, 2015, **54**, 7837-7841.
- 85. P. Chuentragool, M. Parasram, Y. Shi and V. Gevorgyan, *J. Am. Chem. Soc.*, 2018, **140**, 2465-2468.
- 86. F. W. Friese, C. Muck-Lichtenfeld and A. Studer, *Nat. Commun.*, 2018, **9**, 2808.
- 87. (a) K. A. Margrey, W. L. Czaplyski, D. A. Nicewicz and E. J. Alexanian, *J. Am. Chem. Soc.*, 2018, **140**, 4213-4217; (b) A. Hu, J.-J. Guo, H. Pan and Z. Zuo, *Science*, 2018, **361**, 668-672; (c) S. Mukherjee, B. Maji, A. Tlahuext-Aca and F. Glorius, *J. Am. Chem. Soc.*, 2016, **138**, 16200-16203.
- 88. J. C. Scaiano and L. C. Stewart, *J. Am. Chem. Soc.*, 1983, **105**, 3609-
- 89. A. Clerici, R. Cannella, W. Panzeri, N. Pastori, E. Regolini and O. Porta, *Tetrahedron Lett.*, 2005, **46**, 8351-8354.
- 90. B. Ye, J. Zhao, K. Zhao, J. M. McKenna and F. D. Toste, *J. Am. Chem. Soc.*, 2018, **140**, 8350-8356.
- 91. Z. Liu, M. Li, G. Deng, W. Wei, P. Feng, Q. Zi, T. Li, H. Zhang, X. Yang and P. J. Walsh, *Chem. Sci.*, 2020, **11**, 7619-7625.
- 92. K. M. Nakafuku, Z. Zhang, E. A. Wappes, L. M. Stateman, A. D. Chen and D. A. Nagib, *Nat. Chem.*, 2020, **12**, 697-704.

# **TOC Graphic**

